



HAL
open science

Release and toxicity of adipose tissue-stored TCDD: Direct evidence from a xenografted fat model

Nolwenn Joffin, Philippe Noirez, Jean-Philippe Antignac, Min-Ji Kim,
Philippe Marchand, Marion Falabrègue, Bruno Le Bizec, Claude Forest,
Claude Emond, Robert Barouki, et al.

► **To cite this version:**

Nolwenn Joffin, Philippe Noirez, Jean-Philippe Antignac, Min-Ji Kim, Philippe Marchand, et al..
Release and toxicity of adipose tissue-stored TCDD: Direct evidence from a xenografted fat model.
Environment International, 2018, 121, pp.1113-1120. 10.1016/j.envint.2018.10.027 . hal-01922515

HAL Id: hal-01922515

<https://hal.science/hal-01922515>

Submitted on 14 Nov 2018

HAL is a multi-disciplinary open access archive for the deposit and dissemination of scientific research documents, whether they are published or not. The documents may come from teaching and research institutions in France or abroad, or from public or private research centers.

L'archive ouverte pluridisciplinaire **HAL**, est destinée au dépôt et à la diffusion de documents scientifiques de niveau recherche, publiés ou non, émanant des établissements d'enseignement et de recherche français ou étrangers, des laboratoires publics ou privés.

1
2
3 **1. Title page**
4

5 **2 Manuscript title: Release and toxicity of adipose tissue-stored TCDD: direct evidence from a**
6 **3 xenografted fat model**
7
8

9
10 **4**
11 **5 Names of the authors:** Nolwenn Joffin^{1,2*}, Philippe Noirez^{1,2,3,4,5*}, Jean-Philippe Antignac⁶, Min-ji
12 Kim^{1,6}, Philippe Marchand⁷, Marion Falabregue^{2,3,4}, Bruno Le Bizec⁷, Claude Forest^{1,2}, Claude
13 Emond^{5,8,9}, Robert Barouki^{1,2}, Xavier Coumoul^{1,2}
14
15

16 **8 Equal contributions (*) :** Philippe Noirez and Nolwenn Joffin
17

18 **9 Affiliations of all authors** (department, institution, city, state/province, and country)
19

20
21 ¹ INSERM UMR-S1124, Toxicologie Pharmacologie et Signalisation cellulaire
22

23 ² Université Paris Descartes, 45 rue des Saints-Pères, 75006 Paris, Sorbonne Paris Cité, Paris,
24 France
25

26 ³ IRMES, EA 7329, Institut de Recherche bioMédicale et d'Epidémiologie du Sport, Paris, France
27

28 ⁴ Institut National du Sport, de l'Expertise et de la Performance (INSEP), Paris, France
29

30 ⁵ Université du Québec à Montréal (UQAM), Montreal, Qc, Canada
31

32 ⁶ Université Paris 13, Sorbonne Paris Cité, Bobigny, France
33

34 ⁷ Laboratoire d'Etude des Résidus et Contaminants dans les Aliments (LABERCA), UMR 1329 Oniris-
35 INRA, Nantes, France
36

37 ⁸ BioSimulation Consulting Inc, Newark, DE, USA, 19713
38

39 ⁹ Université de Montréal, Montreal, Qc, Canada
40

41 **22 Name of and contact information for corresponding authors:** X. Coumoul^{1,2}; phone:
42 +33142863359; fax: +33142863868; email: xavier.coumoul@parisdescartes.fr; R. Barouki^{1,2};
43 phone: +33142862075; fax: +33142863868; email: robert.barouki@parisdescartes.fr
44

45 **25 Running title:** PBPK model describing POPs release by fat tissue
46
47

48 **27 Acknowledgments and funding:** This work was supported by the ANSES (ALLOFATOX-Funding
49 including PhD fellowship: N. Joffin), the Université Paris Descartes-COMUE-SPC (Funding), INSERM
50 (Funding), Assistance Publique-Hôpitaux-de-Paris, the LUNAM Université (Funding).
51
52

53 **30 A competing financial interest's declaration:** all authors have disclosed that there is no actual or
54 potential competing interest regarding the submitted article
55
56
57
58
59

60
61
62
63
64
65
66
67
68
69
70
71
72
73
74
75
76
77
78
79
80
81
82
83
84
85
86
87
88
89
90
91
92
93
94
95
96
97
98
99
100
101
102
103
104
105
106
107
108
109
110
111
112
113
114
115
116
117
118

32

33
34
35
36
37
38
39
40
41
42
43
44

45

46

47
48
49
50

51

52

List of abbreviations: alpha-SMA: alpha-smooth muscle actin; AhR: aryl hydrocarbon receptor; AQP: aquaporin; AT: adipose tissue; ATGL: adipose triglyceride lipase; bw: body weight; CD: cluster of differentiation; COL1A1: collagen 1A1; CPT1B: carnitine palmitoyl-transferase 1B; CYP: cytochrome P450; FABP4: fatty acid binding protein 4; FAS: fatty acid synthase; G6Pase: glucose-6 phosphatase; HSL: hormone-sensitive lipase; IL: interleukin; MCP-1: monocyte chemoattractant protein-1; NOS2: NO Synthase 2; PAI-1: plasminogen activator inhibitor-1; PBPK: Physiologically based pharmacokinetic; PC: pyruvate carboxylase; PCB: polychlorinated biphenyl; PDK: pyruvate dehydrogenase kinase; PECK: phosphoenolpyruvate carboxykinase; PGC-1 alpha: PPARγ-coactivator 1 alpha; POPs: Persistent Organic Pollutants; PPARα: peroxisome proliferator-activated receptor-alpha; PPARγ2: PPAR-gamma2; RT-qPCR: real-time quantitative PCR; SD: Standard Deviation; TNF: Tumor-Necrosis Factor; UCP1: uncoupling protein 1; VLCAD: Very long-chain acyl-CoA dehydrogenase; PBPK: Physiologically Based Pharmacokinetic.

Highlights

- A new model to study the release and distribution of POPs
- Introduction of a new PBPK model to study the effects of POPs
- Internal release of TCDD activates signatures of inflammation & fibrosis.
- Internal stores of POPs could play a significant role in long term toxicity.

119
120
121
122
123
124
125
126
127
128
129
130
131
132
133
134
135
136
137
138
139
140
141
142
143
144
145
146
147
148
149
150
151
152
153
154
155
156
157
158
159
160
161
162
163
164
165
166
167
168
169
170
171
172
173
174
175
176
177

53 **2. Abstract.**

54 **Background:** Persistent organic pollutants (POPs) are known to accumulate in adipose tissues (AT).
55 This storage may be beneficial by diverting POPs from other sensitive tissues or detrimental because
56 of chronic release of pollutants as indirectly suggested during weight loss. The aim is to study the
57 biological and/or toxic effects that chronic POP release from previously contaminated grafted AT could
58 exert in a naïve mouse. **Methods:** C57BL/6J male mice were exposed intraperitoneally to 2,3,7,8-
59 tetrachlorodibenzo-p-dioxin (TCDD); their epididymal fat pads were collected and grafted on the back
60 skin of uncontaminated recipient mice whose brain, liver, and epididymal ATs were analyzed (TCDD
61 concentration, relevant gene expression). Kinetics of release and redistribution were modeled using
62 Physiologically Based Pharmacokinetics (PBPK). **Results:** The grafts released TCDD over a period of 10
63 weeks with different kinetics of distribution in the three organs studied. A PBPK model was used to
64 simulate the AT releasing process and the incorporation of TCDD into the major organs. At three weeks
65 post-graft, we observed significant changes in gene expression in the liver and the host AT with
66 signatures reminiscent of inflammation, gluconeogenesis and fibrosis as compared to the control.
67 **Conclusions:** This study confirms that AT-stored TCDD can be released and distributed to the organs
68 of the recipient hence leading to distinct changes in gene expression. This original model provides
69 direct evidence of the potential toxic-relevant effects when endogenous sources of contamination are
70 present.

71

72 **Keywords:** adipose tissue, graft, internal release, dioxin, TCDD, PBPK, fibrosis

73

178
179
180 **74 3. Introduction**
181

182 75 Persistent organic pollutants (POPs) are xenobiotics of major concern for environmental health
183 76 (Bonde et al., 2016; Mostafalou, 2016; Smarr et al., 2016). 2,3,7,8-tetrachlorodibenzo-p-dioxin (TCDD)
184 77 is one of the most potent compounds among the dioxin class of substances and its toxicity equivalence
185 78 factor is set to a reference value of 1. TCDD binds to the Aryl hydrocarbon Receptor (AhR), a protein of
186 79 the basic Helix-Loop-Helix / Per - ARNT - Sim (bHLH/PAS) family, which transcriptionally activates the
187 80 expression of genes which code for xenobiotic metabolizing enzymes (XME) as well as that of other
188 81 genes (Guyot *et al.* 2013). However, in spite of the induction of these detoxifying enzymes, the TCDD
189 82 and other POPs are very poorly metabolized and, therefore, not readily eliminated. This, as well as
190 83 their lipophilicity, accounts for their accumulation in adipose tissue (AT) (Lee *et al.* 2017).
191

192 84 The storage of POPs in AT is believed to have complex implications and consequences (Kim *et*
193 85 *al.* 2011, 2012). It may be protective to a certain extent since it diverts POPs from critical target organs
194 86 such as the brain. However, it is also assumed that contaminated AT progressively delivers POPs that
195 87 would eventually lead to a chronic low-rating release resulting in chronic toxicity. Indeed, we and
196 88 others observed an increase in blood POPs following weight loss (Chevrier *et al.* 2000, Imbeault *et al.*
197 89 2002, Kim *et al.* 2011) but such increase could also be the result of the dynamic switch between
198 90 lipolysis and lipogenesis that occurs during fasting/feeding process, independent of weight loss. The
199 91 evidence for both scenarios, *i.e.* protection and long-term toxicity, is indirect at this stage.
200

201 92 Long-term exposure to TCDD has been associated with many pathologies including cancer,
202 93 infertility or metabolic diseases (White and Birnbaum, 2009). Its carcinogenic effects have been
203 94 established by the World Health Organization (WHO) and the US National Toxicology Program (NTP)
204 95 despite some conflicting results in humans (Boffetta *et al.* 2011). Regarding metabolic diseases, a
205 96 recent meta-analysis pointed to a likely link between TCDD exposure and type 2 diabetes (Goodman
206 97 *et al.* 2015), while *in vitro* and *in vivo* experiments showed that TCDD reduced glucose uptake by the
207 98 liver and AT, a process that occurs with decreases in insulin production and secretion by beta-
208 99 pancreatic cells (Novelli *et al.* 2005). TCDD is also suspected to elicit metabolic diseases through either
209 100 the induction of local inflammation of the AT (Kim *et al.* 2012), the regulation of endogenous
210 101 metabolizing enzymes (carbohydrate and lipid pathways) (Ambolet-Camoit *et al.* 2015) or epigenetic
211 102 mechanisms. Such TCDD effects are consistent with the suspected obesogen effects of several POPs
212 103 (*i.e.* organochlorinated pesticides) (La Merrill *et al.* 2013; Lee *et al.* 2014).
213
214
215
216
217
218
219
220
221
222
223
224
225
226
227
228

229 104 While the long-term toxicity of TCDD (and other POPs) is now established, there is still no direct
230 105 evidence that its release from AT is involved in such long-term toxicity although such effects are being
231 106 suspected (Kim *et al.* 2011). In all experimental protocols, animals are either fed or injected with TCDD,
232
233
234
235
236

237
238
239
240
241
242
243
244
245
246
247
248
249
250
251
252
253
254
255
256
257
258
259
260
261
262
263
264
265
266
267
268
269
270
271
272
273
274
275
276
277
278
279
280
281
282
283
284
285
286
287
288
289
290
291
292
293
294
295

107 resulting in single (or repetitive) exposures. There are several possible mechanisms for long-term
108 toxicity. Such toxicity may be due to the direct effect of ingested TCDD following exposure but could
109 also be additionally due to TCDD output from internal compartments like AT. Because of the lack of an
110 experimental model assessing the role of AT-stored TCDD, it has not been possible yet to assess those
111 hypotheses and to clearly identify the kinetic and dynamic behaviors of TCDD discharged from internal
112 storage sites.

113 The aims of the present study were 1) to develop an experimental model based on a surgical
114 graft procedure; 2) to describe the fate and effects of AT-stored TCDD then specifically investigate
115 whether this compound can be discharged from the AT and display activity on other tissues, and 3) to
116 build a physiologically based pharmacokinetic (PBPK) model to simulate the distribution of TCDD by
117 gavage and the donor, and then at the second time simulating a chronic endogenous POP release from
118 the graft implant in the host, and 4) to characterize the effects of this release on the expression of
119 several biomarkers linked to pathologies. To achieve this goal, we have developed a unique, new and
120 original experimental model allowing such investigation. We have grafted TCDD-contaminated AT to
121 uncontaminated mice and monitored the action that sub-chronic release of this POP could exert in
122 three host tissues, AT, liver and brain; such novel bioengineered mice allowed the generation of a PBPK
123 model simulating a chronic POP output from a grafted implant. We characterized the effects of this
124 release on the expression of several biomarkers linked to the above-described pathologies - including
125 endogenous metabolic enzymes or inflammatory cytokines - in recipient AT and liver, two organs that
126 are critically involved in metabolic regulations.

127

296
297
298
299
300
301
302
303
304
305
306
307
308
309
310
311
312
313
314
315
316
317
318
319
320
321
322
323
324
325
326
327
328
329
330
331
332
333
334
335
336
337
338
339
340
341
342
343
344
345
346
347
348
349
350
351
352
353
354

128 **4. Materials and Methods**

129 **4.1 Mice**

130 The European Communities Council Directive 2010/63/EU on the protection of the animals
131 was followed for the experiments using animals. All procedures were approved by the ethical
132 committee for animal research of Paris Descartes university (CEEA.34, number: 12-132). C57BL/6J
133 male mice (12-week-old) with body weight (bw) about 25 g were obtained from Janvier and allowed 1
134 week to acclimate at the Paris Descartes university animal facility before the study. Animals were
135 maintained on a 12-hr light/dark cycle at the ambient temperature of a $22 \pm 1^\circ\text{C}$ and relative humidity
136 of $55 \pm 5\%$ and were provided with Purina 5001 rodent Chow (Safe) and tap water ad libitum.

138 **4.2 Primary POPs exposure**

139 The mice donor C57BL/6J received a single intraperitoneal injection with either dose of 0, 1,
140 10 or 25 μg TCDD/kg of bw in corn oil. Mice were sacrificed 48h after injection. For each mouse, both
141 epididymal fat pads were collected: one was used for TCDD quantification and the other for the graft
142 to a donor mouse.

144 **4.3 Graft of epididymal AT contaminated with POPs**

145 Each epididymal fat pad was grafted into the subcutaneous plane on the back of the mice.
146 Mice were sacrificed at 0.5, 1, 2, 3, 4 or 10 weeks following the graft. The graft, brain, liver, and
147 epididymal AT were removed for quantification of TCDD and gene analyses. We observed that the
148 grafts were revascularized between 4 and 10 weeks following the surgical procedure (data not shown).

150 **4.4 POPs internal exposure levels quantification**

151 The methodology that was applied to isolate, detect, and quantify TCDD had its origin in a
152 more global previously described method used for measuring dioxins and PCBs (Costera et al. 2006).
153 Briefly, ^{13}C -labelled TCDD was added to each sample for quantification according to the isotopic
154 dilution method. Samples of AT (50 to 250 mg), liver (0.150 to 1.750 g) and brain (150 to 550 mg) were
155 first submitted to an accelerated solvent extraction at high temperature and high pressure (ASE
156 Dionex, Sunnyvale, CA). The resulting extracts were weighed to evaluate fat content by a gravimetric
157 method and were reconstituted in hexane for further sample clean up through three purification steps
158 using successively acid silica, florisil, and celite/carbon columns. TCDD concentrations were assessed
159 using gas chromatography (Agilent 7890A) coupled to high-resolution mass spectrometry (GC-HRMS)
160 on electromagnetic sector instrument (JEOL MS 800D), operating at 10,000 resolutions and in the
161 single ion monitoring (SIM) acquisition mode. This method was validated according to current

355
356
357
358
359
360
361
362
363
364
365
366
367
368
369
370
371
372
373
374
375
376
377
378
379
380
381
382
383
384
385
386
387
388
389
390
391
392
393
394
395
396
397
398
399
400
401
402
403
404
405
406
407
408
409
410
411
412
413

162 European criteria in the field of regular control of foodstuff of animal origin and accredited according
163 to the ISO 17025 standard.

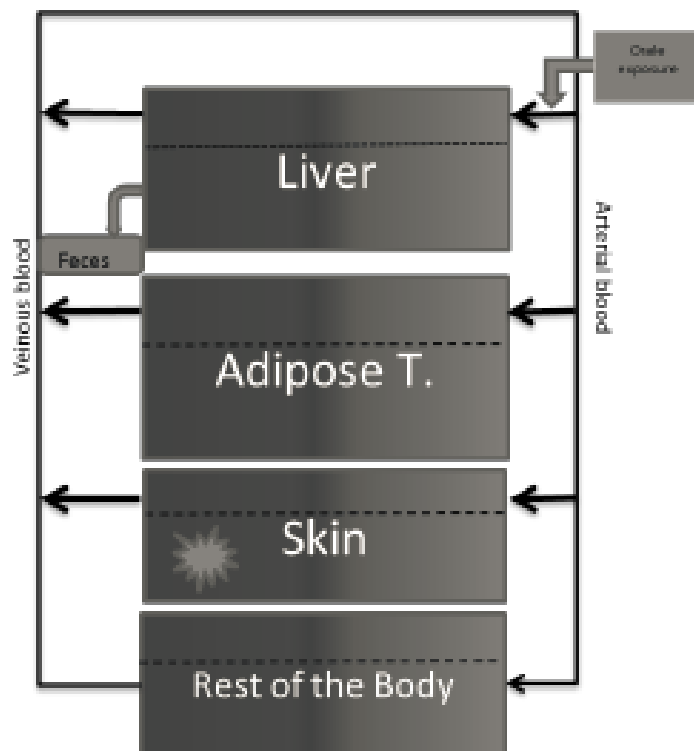
164

165 **4.5 PBPK modeling**

166 Several models have been published to mimic the pharmacokinetics of TCDD on different
167 species (Emond, 2004; Kissel and Robarge, 1998; Leung et al., 1990, 1988). More recently, a PBPK
168 model for TCDD has been applied to humans and mice (Emond et al., 2010; Emond et al., 2016) to
169 study the influence of obesity and diabetes on the elimination of TCDD (Emond et al., 2018). A larger
170 description and assessment work of the PBPK model for mice were performed and peer-reviewed
171 during the NCEA-USEPA reassessment (USEPA, 2012). This version of the PBPK model was used as a
172 base for the present work. Briefly, the model is originally composed of 3 compartments (liver, AT and
173 the rest of the body) connected to the systemic circulation (arterial and venous). The rest of the body
174 compartment is composed of muscles ($\approx 70\%$) and other non-essential organs for the pharmacokinetics
175 but is required for the mass balance calculation. The rest of the body is then described as permeability-
176 limited compartments (composed of extracellular matrix and blood sub-compartments). The
177 elimination of TCDD from the body is very limited; it happens mostly in the feces and not much in the
178 urine. In addition, the PBPK model also integrates an enterohepatic cycle; overall, it allows the
179 description of an elimination rate based on the body burden using a mathematical component function
180 (Emond et al. 2016; USEPA 2012). One key parameter of this model, which conditions the elimination
181 rate of TCDD, is the induction of CYP1A2 which is due to AhR activation (CY1A2 is a transcriptional
182 target of the AhR) which depends on the body burden (Diliberto et al. 1997; Emond et al. 2005, 2006).
183 All the parameters used in this PBPK model, before modification, were previously assessed and
184 presented in the USEPA 2012 report (in this reference, see Tables 3-8 pages 3-63).

185 To describe the release of TCDD from the AT implanted in the dorsal subcutaneous skin region
186 (graft), it was necessary to update the original PBPK model by adding a skin compartment and graft
187 (Figure 1).

414
415
416
417
418
419
420
421
422
423
424
425
426
427
428
429
430
431
432
433
434
435
436
437
438
439
440
441
442
443
444
445
446
447
448
449
450
451
452
453
454
455
456
457
458
459
460
461
462
463
464
465
466
467
468
469
470
471
472



188

Figure 1: Conceptual representation of the PBPK model in mice

189

Indeed, we assumed that the graft was an entity added to the skin compartment. Basically, the graft releases the TCDD which diffuses to the skin compartment and is then released in the blood. The blood flow in the skin compartment was described as permeability-limited; all parameters for this additional compartment including the partition coefficient "skin/ blood" (unitless), perfusion of the skin compartment ($\text{ml}\cdot\text{h}^{-1}$), the diffusion permeability of the skin ($\text{ml}\cdot\text{h}^{-1}$) and the volume of skin tissue (ml) were extracted from the literature (Brown *et al.*, 1997; Wang *et al.*, 1997) (Table 1).

196

197

198 **Table 1: physiological parameters used to define both skin and graft compartments used in the PBPK**
 199 **allografted mice model**

Parameters	Name of the parameters	values	references
V_{sk}	Fraction of body weight for skin (unitless)	0.165	Brown <i>et al.</i> , 1997
V_{skb}	Fraction of tissue blood volumes for skin (unitless)	0.0159	Wang <i>et al.</i> , 1997
Q_{skf}	Tissue blood flow fraction of cardiac output for skin (unitless)	0.057	Brown <i>et al.</i> , 1997
$P_{sk/b}$	Partition coefficient (skin/blood) (unitless)	10	Wang <i>et al.</i> , 1997
KGRAFT	First order parameter of TCDD release in graft to the skin (h^{-1})	0.004	Optimized
PASKINF	Diffusion permeability (unitless)	0.09	Optimized
R	Fraction of blood diffusion (PASKIN) from the blood skin to the grafted starting 4 weeks post graft implantation (unitless)	R= 0.0007	Optimized

200
 201 The graft sub-compartment is essentially composed of TCDD-delivering AT (see §4.2). This
 202 delivery was estimated using the concentration of TCDD in the graft at time 0 and the subsequent
 203 measurements at different time points (using a first order kinetic release of TCDD from the graft to the
 204 skin). We also consider a functional vascularization of the graft around week 4 (visual observation).
 205 The parameters used to mimic mathematically the release of TCDD from the graft are presented in
 206 Table 2:

208 **Table 2: Parameters used to mimic mathematically the release of TCDD from the graft in the**
 209 **corresponding equations**

Parameters	Description of the parameters
cgraft0	concentration of TCDD in the graft at time 0 ($pg.g^{-1}$)
graftmass	mass of the graft (g)
agraftpg	amount of TCDD at time 0 (pg)
kgraft	constant transfer of TCDD from graft to skin (h^{-1})
agraftng	amount of TCDD in the graft at time 0 (ng)
agraftnmol	amount of TCDD in the graft at time 0 (nmole)
agraftresnmol	amount of TCDD remaining in the graft at different time points (nmole)

532
533
534
535
536
537
538
539
540
541
542
543
544
545
546
547
548
549
550
551
552
553
554
555
556
557
558
559
560
561
562
563
564
565
566
567
568
569
570
571
572
573
574
575
576
577
578
579
580
581
582
583
584
585
586
587
588
589
590

211 The amount of TCDD which remains in the graft after each time point (dt), also *agraftresnmol*,
212 was estimated using **equation 1**:

- **Equation 1:** variation of the amount of TCDD (nmole) that remains in the graft after each time interval (dt) in hours

$$\frac{d\text{agraftnmol}(\text{nmol})}{dt(\text{h})} = -k\text{graft} \times \text{agraftresnmol}$$

219 Then, the changes in TCDD concentrations in the grafts were estimated using **equations 2 & 3**.

- **Equation 2** Amount of TCDD (nmoles) remaining in the graft after each time point (dt):

$$\text{agraftresnmol} = \int_{t-1}^t \text{agraftnmol}$$

- **Equation 3:** Concentration of TCDD in pg/g

$$\text{agraftrespgg}\left(\frac{\text{pg}}{\text{g}}\right) = \text{agraftresnmol}(\text{nmole}) \times \frac{MW\left(\frac{\text{ng}}{\text{nmole}}\right) \times 1000\left(\frac{\text{pg}}{\text{ng}}\right)}{\text{graftmass}(\text{g})}$$

228 These simulation parameters were optimized by a first series of experiments carried out to
229 assess the release of TCDD from the graft during the optimization of the exposure dose of the donor.
230 Determination of the graft mass and the concentration of TCDD at different time points were
231 compared to the simulation profile resulting from the model. In addition, simulation of TCDD
232 generated using the PBPK model was compared to the experimental time points determined
233 experimentally.

4.6 RNA sampling from tissues

236 AT and liver samples were placed in 1 mL of Qiazol® reagent with 2 stainless steel beads
237 (Qiagen, France) and were homogenized with a TissueLyser system (RetschMM300, Germany). Total
238 RNA was prepared using the RNeasy Mini Kit following the manufacturer's instructions (Qiagen,
239 France). The quality of total RNA was monitored with a Nanodrop ND-1000 spectrophotometer
240 (Nanodrop products, Wilmington, USA).

591
592
593 **248 4.7 Quantitative real-time PCR**
594

595 **249** Reverse transcription was carried out using the High Capacity cDNA Reverse Transcription Kit
596 (Life technology, France) according to the manufacturer's directions. Real-time PCR was achieved with
597 **250**
598 **251** 20 ng of cDNA, with duplicates for each experiment. STable 1 (Suppl Mat.) gives the gene-specific
599
600 **252** primers. The relative amounts of mRNA were estimated using the $\Delta\Delta C_T$ method with Ribosomal Protein
601 **253** L13 (RPL13) as the reference gene (Juricek *et al.*, 2014; Pfaffl, 2001).
602
603 **254**

Gene	Forward primer	Reverse primer
AhR	ACAGTAAAGCCCATCCCC	AGCACAAAGCCATTTCAGC
CYP1A1	ATGAGTTTGGGGAGGTTACTG	AATGAGGCTGTCTGTGATGTC
CYP1B1	GAGGATGTGCCTGCCACTA	CTGTGGCTGCTCATCCTCTT
IL-1 β	GCCACCTTTTGACAGTGATG	TCTCCACAGCCACAATGAG
IL-6	CTTCCATCCAGTTGCCTTCTTG	AATTAAGCCTCCGACTTGTGAAG
TNF alpha	TCATCCATTCTCTACCCAGC	GTCCCAGCATCTTGTGTTTC
MCP-1	AGCAGCAGGTGTCCCAAAGA	ACGGGTCAACTTCACATTCAA
NOS2	TGAGGGGACTGGACTTTTAG	CTGTGACTTTGTGCTTCTGC
F4/80	TTTCTCGCCTGCCTCTTC	CCCCGTCTCTGTATTCAACC
COL1A1	TCATCGTGGCTTCTCTG	CGTTGAGTCCGTCTTTG
Alpha-SMA	CCTGGTGTGCGACAATG	TGCTCTGGGCTTCATCC
Glycogen synthase 2	CCAGCTTGACAAGTTCGACA	ATCAGGCTTCTCTTCAGCA
PC	CGGCAGGGCGGAGCTAACAT	TTTGGGGAGGCAACAGGGGC
PEPCK-c	AGTGCCCCATTATTGACC	TCTTGCCCTTGTGTTCTG
G6Pase	CCAAGGGAGGAAGGATG	AGGTGACAGGGAAGTCT
PGC-1 alpha	TGCCCTGCCAGTCACAGGA	GCTCAGCCGAGGACACGAGG
RPL13	GGATCCCTCCACCCTATGACA	CTGGTACTTCCACCCGACCTC
CD68	CCAATTCAGGGTGAAGAAA	CTCGGGCTCTGATGTAGGTC
AQP7	GAAGTCAAGGCTTGGTCTGCT	CATGTGAGCCACGGAACCAA
ATGL	CCAACGCCACTCACATC	CAGAGGACCCAGGAACC
HSL	ACTGAGATTGAGGTGCTGTC	AAGGCAGGTGAGATGGTAAC
CPT1B	TTCCGACAAACCCTGAAGCT	TAAGATCTGGGCTATCTGTGTC
VLCAD	TGAATGACCCTGCCAAG	CCACAATCTCTGCCAAGC
CD36	CATGAGAATGCCTCCAAACAC	GGAAGTGTGGGCTCATTGC
GLYCOGEN KINASE	ATCCGCTGGCTAAGAGACAACC	TGCACTGGGCTCCCAATAAGG
PDK4	TGTGATGTGGTAGCAGTAGTC	ATGTGGTGAAGGTGTGAAG
FABP4	AACACCGAGATTTCTT	ACACATTCCACCACCAG
PPAR α	AAGCCATCTTCACGATGCTG	TCAGAGGTCCCTGAACAGTG
FAS	TCCTGGGAGGAATGTAAACAGC	CACAAATTCATTACTGCAGCC
UCP1	CCGCGACTTCGGACTCCTGC	TAACGGGTCTCCCTGCCCG
PPAR γ 2	TTATGCTGTTATGGGTGAAA	CAAAGGAATGCGAGTGGTC

644 **255**
645 **256** **Supplementary table S1: list of primers used for quantitative RT-PCR experiments**
646
647
648
649

650
651
652
653
654
655
656
657
658
659
660
661
662
663
664
665
666
667
668
669
670
671
672
673
674
675
676
677
678
679
680
681
682
683
684
685
686
687
688
689
690
691
692
693
694
695
696
697
698
699
700
701
702
703
704
705
706
707
708

257
258
259
260
261
262
263

4.8 Statistical analyses

Unless otherwise specified, two-group and multiple-group comparisons were made using Mann-Whitney's U-test (nonparametric comparison of two independent series) or Kruskal-Wallis test followed by a pair-wise Dunn's post hoc test (nonparametric comparison of multiple independent series). A p-value < 0.05 was considered statistically significant (** p<0.01, * p<0.05). The values are expressed as the mean ± standard deviation.

709
710
711 264 **5. Results**

712
713 265 **5.1 Xenografted-adipose tissue releases TCDD**

714
715 266 Vehicle (control) or three different doses of TCDD (1, 10 or 25 $\mu\text{g}\cdot\text{kg}^{-1}$ bw; corn oil as a control)
716 267 were intraperitoneally injected to C57BL6/J male mice that were sacrificed 48h later. TCDD
717 268 concentration was determined in the epididymal AT of control (corn oil) and exposed mice, showing a
718 269 proportional increase in the TCDD levels in line with the injected doses (STable 2, Suppl. Mat.).

720
721
722

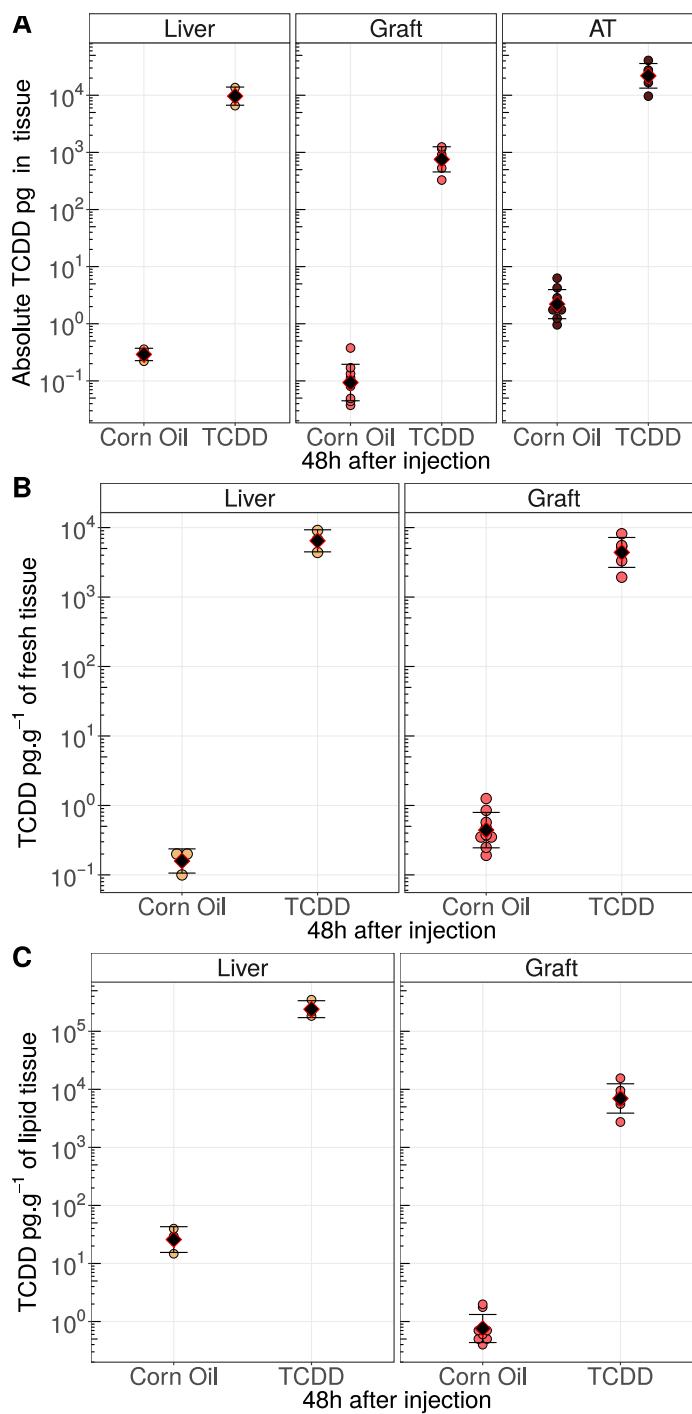
TCDD dose ($\mu\text{g}\cdot\text{kg}^{-1}$ bw)	Levels of TCDD in the AT 48h later ($\text{pg}\cdot\text{g}^{-1}$ fresh tissue)	Relative fold increase in the AT
0	6	-
1	2 335	1
10	21 623	9
25	56 608	24

723
724
725
726
727
728
729
730
731
732

733 270
734 271 **Supplementary table S2: comparison of TCDD-injected doses ($\mu\text{g}\cdot\text{kg}^{-1}$ bw) in C57BL/6J male**
735 272 **mice and its levels in the AT ($\text{pg}\cdot\text{g}^{-1}$ fresh tissue) 48h after injection.**

736 272
737 273
738 274
739 275 The dose of 10 $\mu\text{g}\cdot\text{kg}^{-1}$ bw did not saturate the AT since higher concentrations of TCDD in the
740 276 AT were obtained following the injection of 25 $\mu\text{g}\cdot\text{kg}^{-1}$ TCDD; thus, this dose (10 $\mu\text{g}\cdot\text{kg}^{-1}$ bw) was
741 selected for all subsequent experiments (SFigure 1, Suppl Mat.).
742
743
744
745
746
747
748
749
750
751
752
753
754
755
756
757
758
759
760
761
762
763
764
765
766
767

768
769
770
771
772
773
774
775
776
777
778
779
780
781
782
783
784
785
786
787
788
789
790
791
792
793
794
795
796
797
798
799
800
801
802
803
804
805
806
807
808
809
810
811
812
813
814
815
816
817
818
819
820
821
822
823
824
825
826

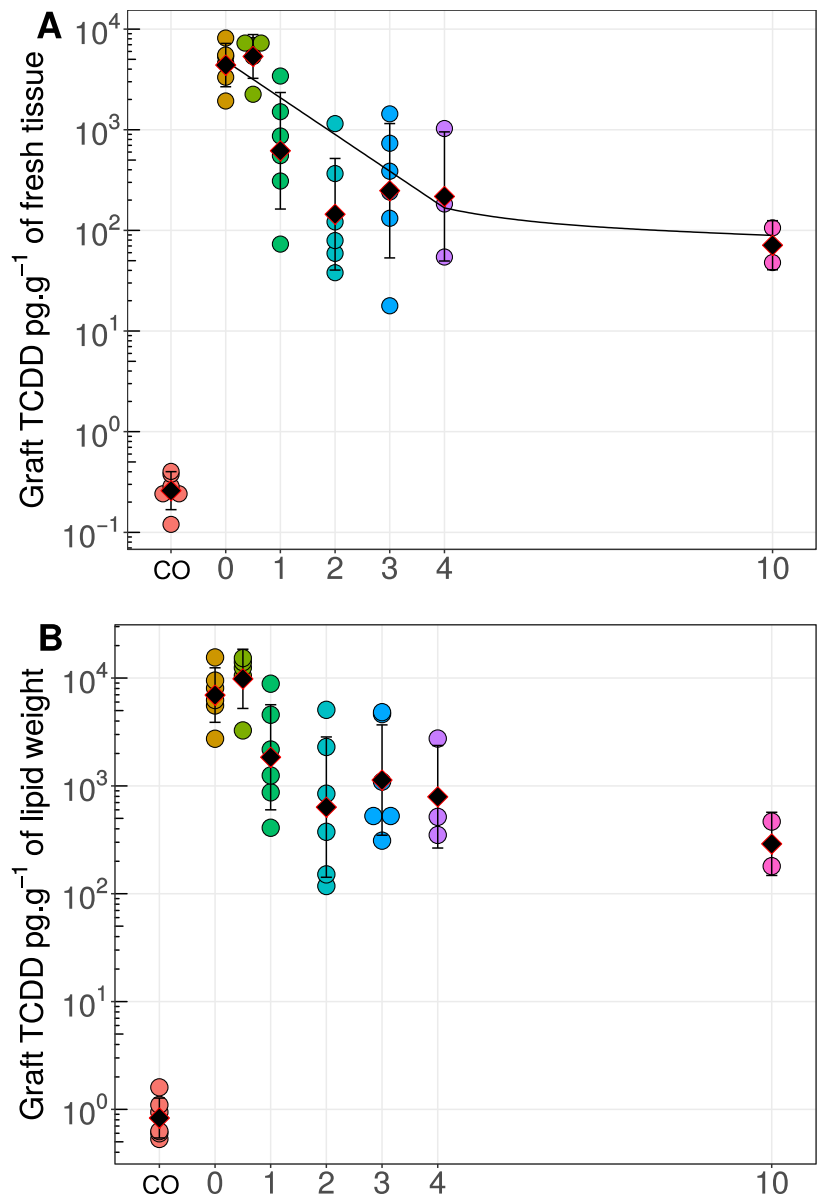


277

278 **Figure 1:** Global burden (pg, A) and concentration levels (pg.g⁻¹ fresh tissue, B and pg.g⁻¹ lipid tissue, C) of TCDD determined in the liver, the graft, and/or the whole AT of the mice donors which had received a single intraperitoneal injection (see §4.2). The levels of TCDD were measured in the liver and the AT; the upper panel represents the absolute quantity (in pg) of TCDD in the liver, the epididymal AT (used later as a graft) and the extrapolated whole-body AT; the middle and lower panels represent the concentration of TCDD (respectively in pg.g⁻¹ of fresh tissue or pg.g⁻¹ of lipids). One of the epididymal AT (the left one) has been used as a graft (weight of the graft: 100-150 mg; approximated concentration of TCDD: 10⁴ pg.g⁻¹ of lipids).

827
828
829
830
831
832
833
834
835
836
837
838
839
840
841
842
843
844
845
846
847
848
849
850
851
852
853
854
855
856
857
858
859
860
861
862
863
864
865
866
867
868
869
870
871
872
873
874
875
876
877
878
879
880
881
882
883
884
885

286 The contaminated AT (epididymal left AT) were then grafted on uncontaminated host C57BL/6J
287 mice. Figure 2 shows that TCDD concentration decreases in the TCDD-contaminated grafted tissue in
288 a time dependent manner.

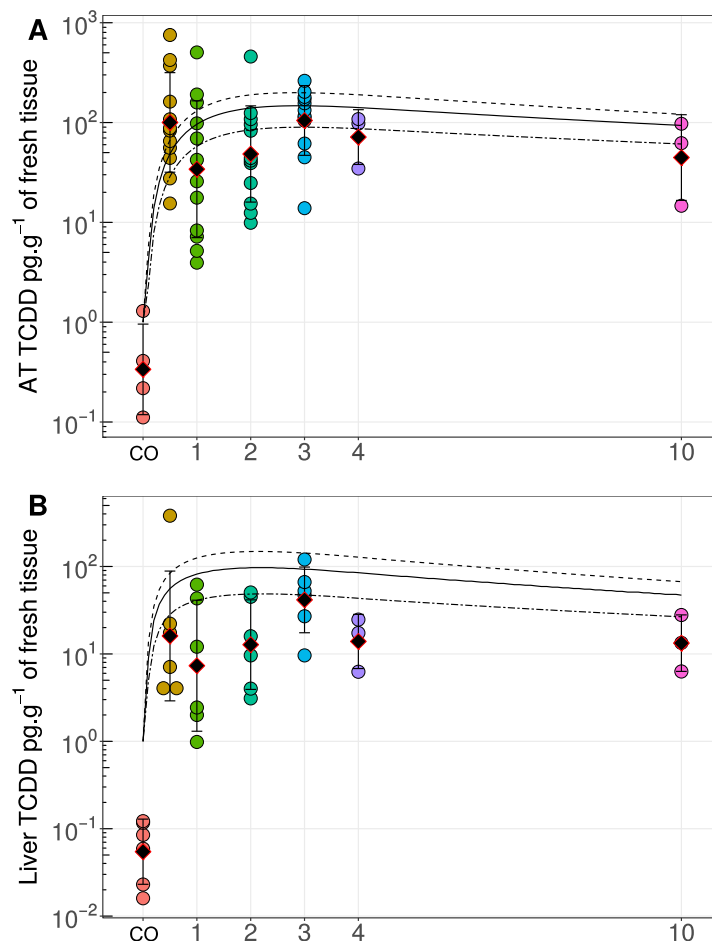


289 **Figure 2:** Levels of TCDD (A: pg.g⁻¹ fresh tissue; B: pg.g⁻¹ lipid weight) measured in the grafted AT (3-6
290 mice/condition) at different time points following the graft (in weeks). The corn oil condition (CO)
291 designates the level of TCDD present in a graft from mice injected with corn oil. In panel A, the line
represents the profiled simulation of TCDD concentrations (expressed in pg TCDD.g⁻¹ fresh tissue) from
the graft implanted in dorsal subcutaneous for 10 weeks.

886
887
888
889
890
891
892
893
894
895
896
897
898
899
900
901
902
903
904
905
906
907
908
909
910
911
912
913
914
915
916
917
918
919
920
921
922
923
924
925
926
927
928
929
930
931
932
933
934
935
936
937
938
939
940
941
942
943
944

292 5.2 TCDD redistributes to other tissues

293 Subsequently, we quantified the distribution of TCDD in three organs of the grafted mice,
294 namely the epididymal AT of the host, liver and brain (respectively figures 3A and 3B, SFigure 2 Suppl.
295 Mat). The levels of TCDD increased significantly in the host AT (figure 3A, from <1 to >100 pg.g^{-1} of
296 fresh tissue in 3 weeks) during the 3-week-time period and remained then stable over the course of
297 the experiments. The distribution in the brain was slower than the distribution in the host AT, with a
298 basal level of 0.1 pg.g^{-1} of fresh tissue and a concentration that reached 1 pg.g^{-1} of fresh tissue at 1
299 week and 10 pg.g^{-1} after 10 weeks (SFigure 2). The levels of TCDD also increased significantly in the
300 liver (figure 3B, from <0.1 to >10 pg.g^{-1} of fresh tissue in 2 weeks) during the 2-week-time period and
301 remained then stable over the course of the experiments.



302 **Figure 3:** Levels of TCDD (pg.g^{-1} of fresh tissue) in the host AT (A), and the liver (B) ($n=6$ mice/condition
303 except weeks 4 and 10) at different time points following the graft (in weeks). For all panels, the
304 symbols (●) represent the individual measurement and the symbols (◆) represents the mean
305 measurement and the standard deviation of the TCDD measured (mean \pm SD) at different time points
306 following the sacrifice. (A) simulation curves of the TCDD accumulation and experimental values in the

AT and (B) in the liver issued from the host following subcutaneous grafting. For each of these tissues, we simulate the mean concentration at time 0, and the concentrations corresponding to the mean \pm SD (see text). The corn oil condition (CO) designates the level of TCDD present in a graft from mice injected with corn oil.

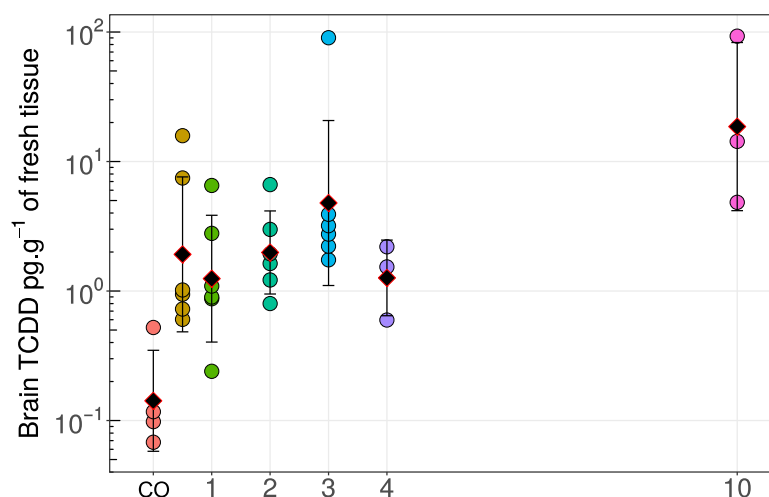


Figure 2: Levels of TCDD (pg.g⁻¹ of fresh tissue) in the brain (n=6 mice/condition except weeks 4 and 10) at different time points following the graft (in weeks). For all panels, the symbols (●) represent the individual measurement and the symbols (◆) represents the mean measurement and the standard deviation of the TCDD measured (mean \pm SD) at different time points following the sacrifice. The corn oil condition (CO) designates the level of TCDD from mice injected with corn oil.

When the levels of TCDD were represented in pg.g⁻¹ of lipid weight (SFigure 3, Suppl. Mat.), a similar profile was obtained for the AT, a tissue with a high fat content. The fast and slow accumulations of TCDD respectively in the liver and the brain were also clearly characterized.

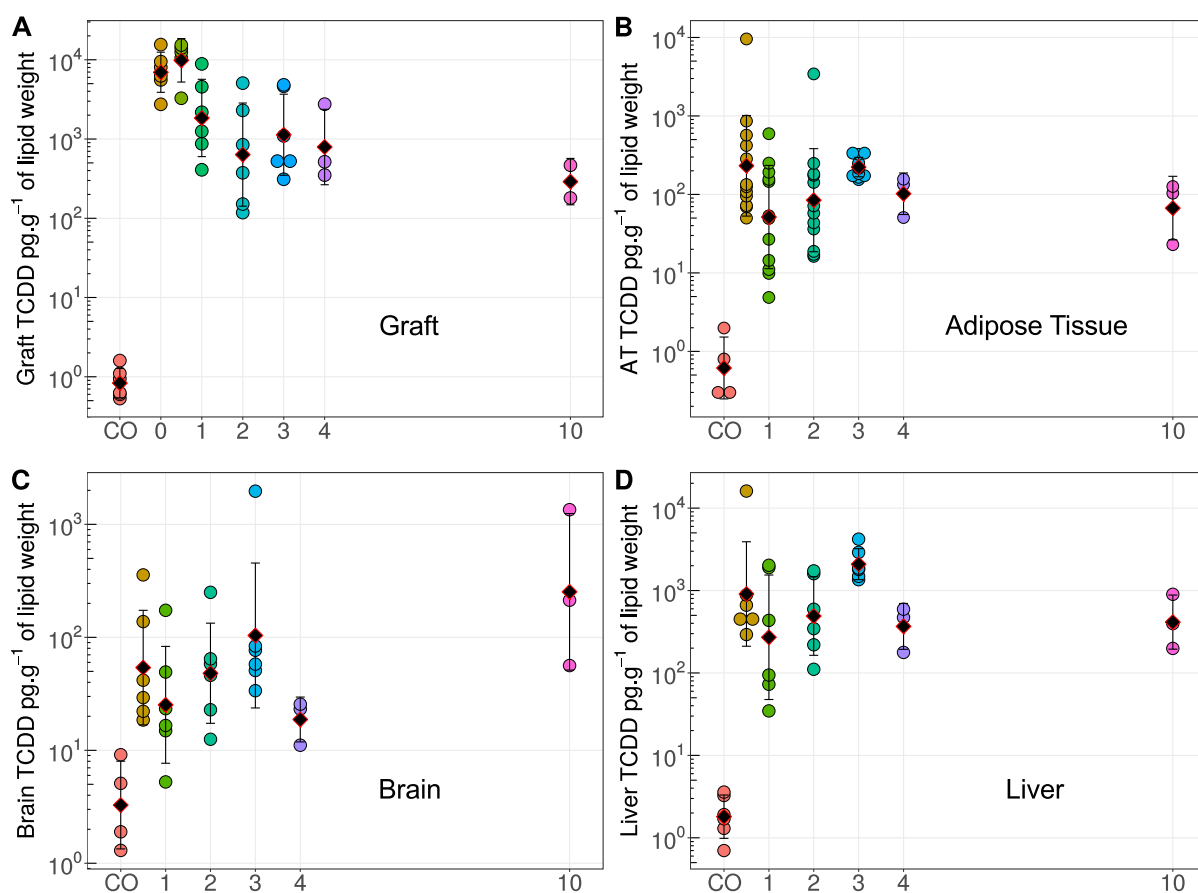


Figure 3: Levels of TCDD ($\text{pg}\cdot\text{g}^{-1}$ lipid weight.) in the graft (A), host AT (B), brain (C) and liver (D) tissues ($n=3-6$ mice/condition) at different time points following the graft (w : weeks). The corn oil condition (CO) designates the level of TCDD present in a graft from mice injected with corn oil.

Overall, our experiments demonstrate that TCDD is quickly released from a contaminated grafted-AT and redistributed in several key organs of the grafted C57BL6 mice albeit with different kinetics.

5.3 PBPK modeling - exposure of the donor

The first step consisted to simulate the exposure of donor mice to a single intraperitoneal injection dose at concentrations of 1, 10 and 25 μg TCDD per kg bw (STable 2, Suppl. Mat.). Using the PBPK mouse model, we simulated the profile of TCDD concentrations in the AT (SFigure 4, Suppl. Mat.).

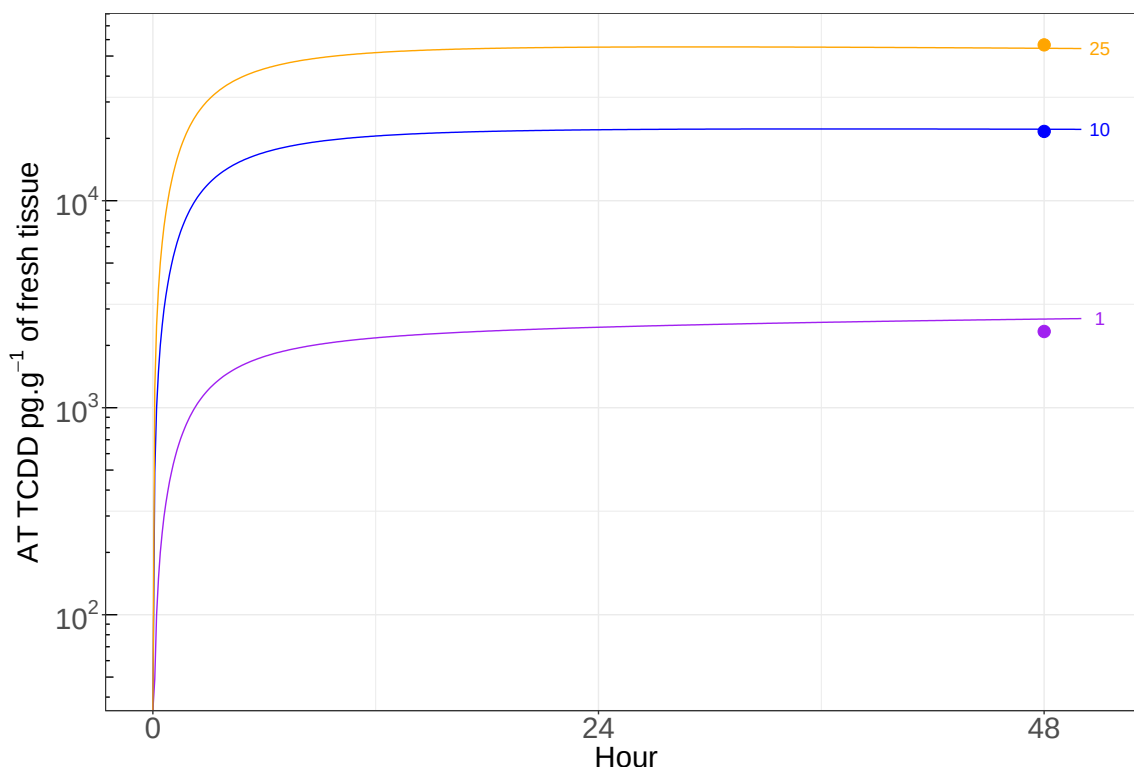


Figure 4: TCDD concentration in mouse AT following a single exposure of TCDD intraperitoneal at 1, 10 or 25 $\mu\text{g.kg}^{-1}$ body weight. The lines depict simulated concentrations and symbols the experimental data at 48h post exposure (see Supplementary table S2).

The simulation matched the experimental measurements of TCDD with very high accuracy (STable 2, Suppl. Mat. and SFigure 4, Suppl. Mat.) and the ratio of the nominal TCDD doses matched well with that of the measured TCDD concentrations in AT (Eq.4).

Equation 4: Comparisons between ratio of dose and tissue concentrations:

$$\frac{\frac{10\mu\text{g}}{\text{kg}}}{1\mu\text{g}/\text{kg}} \cong \frac{\frac{21623\text{pg}}{\text{gtissue}}}{\frac{2335\text{pg}}{\text{gtissue}}} \cong 10 \quad \frac{\frac{25\mu\text{g}}{\text{kg}}}{1\mu\text{g}/\text{kg}} \cong \frac{\frac{56608\text{pg}}{\text{gtissue}}}{\frac{2335\text{pg}}{\text{gtissue}}} \cong 25$$

5.4 PBPK modeling - release of TCDD from the graft / distribution of TCDD in host compartments

The second step consisted of simulating the decrease of TCDD in the graft. Because of the large standard deviations, we used the mean of TCDD concentrations measured in the different assays (4815 pg.g^{-1} fresh tissue at time 0). The first-order elimination rate constant was fixed at 0.004 h^{-1} . The concentration of TCDD in the graft was about 85 pg.g^{-1} fresh tissue at 10 weeks (corresponding to an elimination of 98.23%). The calculated half-life base based on the sequential point was 1.03 weeks on the first part of the biphasic curve (and 5.53 weeks for the second part of the curve).

1122
1123
1124 335 We also simulated the accumulation of TCDD concentrations in the host AT and liver
1125
1126 336 compartments following insertion of the graft. These compartments concentrate more than 90% of
1127 337 the TCDD (Carrier, 1995). However, because the standard deviation (SD) of the initial concentration
1128
1129 338 reflecting the amount of TCDD in the graft was relatively large, the simulation was performed using 1)
1130 339 the mean of the concentrations in the graft, 2) this mean + SD or 3) this mean - SD. Thus, for each
1131
1132 340 compartment, 2 curves were simulated (Figure 3). The prediction of the model was also accurate as
1133 341 the experimental data points for the liver and the AT were found between each maximal and minimal
1134
1135 342 simulating curve (Figure 3).
1136

1137 343 Overall, these two simulations (release and distribution) improved the confidence in the PBPK
1138
1139 344 model for mice.
1140

1141 345 1142 1143 346 **5.5 TCDD release from AT alters the expression of metabolic genes** 1144

1145 347 We next investigated whether the TCDD released from graft-contaminated fat pad could alter
1146 348 expression of genes coding for TCDD-target genes, *i.e.* key biologic or disease-related functions. We
1147 349 and others have previously demonstrated that TCDD induced inflammation and fibrosis in the liver of
1148
1149 350 exposed mice (Duval et al., 2017). Thus, we studied several biomarkers that could be related to chronic
1150 351 liver diseases (*i.e.* fibrosis, steatosis). We carried out RT-qPCR experiments using host liver and AT
1151
1152 352 samples at 3 weeks after grafting.
1153
1154

1155 353 We show that the levels of expression of AhR-target genes in the liver and AT were higher than
1156 354 at time 0, a result in line with a rapid contamination of these organs (Tables 1 and 2). In addition, the
1157 355 expression of fibrotic and inflammatory markers augmented also significantly, in line with our former
1158
1159 356 studies on TCDD treated mice (Duval et al., 2017). The host AT also displayed an inflammatory profile
1160 357 (Table 2).
1161
1162
1163
1164
1165
1166
1167
1168
1169
1170
1171
1172
1173
1174
1175
1176
1177
1178
1179
1180

1181
 1182
 1183 358
 1184
 1185 359
 1186
 1187 360
 1188
 1189 361
 1190
 1191 362
 1192
 1193 363
 1194
 1195 364
 1196
 1197 365
 1198
 1199 366
 1200
 1201 367
 1202
 1203 368
 1204
 1205 369
 1206
 1207 370
 1208
 1209 371
 1210
 1211 372
 1212
 1213 373
 1214
 1215 374
 1216
 1217 375
 1218
 1219 376
 1220
 1221 377
 1222
 1223 378
 1224
 1225
 1226
 1227
 1228
 1229
 1230
 1231
 1232
 1233
 1234
 1235
 1236
 1237
 1238
 1239

Function	Genes	Fold ind.
XME	AhR	2.65
	CYP1A1	8.96**
	CYP1B1	3.62**
Inflammation	IL-1 β	4.17**
	IL-6	1.25
	TNF alpha	1.94
	MCP-1	5.98**
	NOS2	2.42
	F4/80	3.42**
Fibrosis	COL1A1	3.93**
	Alpha-SMA	4.51**
Metabolism	Glycogen synthase 2	3.17**
	PC	3.01**
	Cytosolic PEPCK	2.94**
	G6Pase	2.39**
	PGC-1 alpha	2.24**

Table 1: Relative mRNA level of XME, inflammatory, fibrotic and metabolic marker in the liver following a 3-week internal exposure (statistically significant: ** p<0.01, 6 animals per condition).

1240
 1241
 1242 379
 1243
 1244
 1245
 1246
 1247
 1248
 1249
 1250
 1251
 1252
 1253
 1254
 1255
 1256
 1257
 1258
 1259
 1260
 1261
 1262
 1263
 1264
 1265
 1266
 1267
 1268
 1269
 1270
 1271
 1272
 1273
 1274
 1275
 1276
 1277
 1278
 1279
 1280
 1281
 1282
 1283
 1284
 1285
 1286
 1287
 1288
 1289 380
 1290
 1291 381
 1292 382
 1293 383
 1294
 1295
 1296
 1297
 1298

Function	Genes	Fold ind.
	AhR	0.88
XME	CYP1A1	2.55*
	PAI-1	15.92*
	IL-6	9.4**
	IL10	2.4
Inflammation	TNF alpha	2.01*
	MCP-1	1.83*
	NOS2	1.35*
	CD68	2.79**
	ATGL	1.67*
	HSL	0.66
	CPT1B	1.34
	VLCAD	2.10*
	AQP7	1.23
	CD36	0.49
	Cytosolic PEPCCK	1.24*
Metabolism	Glycerol Kinase	0.06*
	PKD4	3.82*
	PGC-1 alpha	1.18
	FABP4	3.93
	PPAR α	0.85
	FAS	1.74
	UCP1	1.99*
	PPAR γ 2	1.42

Table 2: Relative mRNA expression of several XME, inflammatory, fibrotic and metabolic markers in the AT following a 3-week internal exposure (statistically significant: * p<0.05; ** p<0.01, 6 animals per condition).

1299
1300
1301
1302
1303
1304
1305
1306
1307
1308
1309
1310
1311
1312
1313
1314
1315
1316
1317
1318
1319
1320
1321
1322
1323
1324
1325
1326
1327
1328
1329
1330
1331
1332
1333
1334
1335
1336
1337
1338
1339
1340
1341
1342
1343
1344
1345
1346
1347
1348
1349
1350
1351
1352
1353
1354
1355
1356
1357

384 Due to the role of pyruvate carboxylase (PC), cytosolic phosphoenolpyruvate carboxykinase
385 (PEPCK) and glucose 6 Phosphatase (G6Pase) in maintaining glycemia (potentially linked to type 2
386 diabetes), we investigated the expression of their genes in the liver and found that their mRNA content
387 increased from time 0 to time 3-weeks following grafting.

388
389

1358
1359
1360
1361
1362
1363
1364
1365
1366
1367
1368
1369
1370
1371
1372
1373
1374
1375
1376
1377
1378
1379
1380
1381
1382
1383
1384
1385
1386
1387
1388
1389
1390
1391
1392
1393
1394
1395
1396
1397
1398
1399
1400
1401
1402
1403
1404
1405
1406
1407
1408
1409
1410
1411
1412
1413
1414
1415
1416

390 6. Discussion

391 In the present study we provide direct experimental evidence for the release of TCDD from
392 adipose tissue (AT, graft) and its migration into other tissues. We also show that the released pollutant
393 induces relevant changes in gene expression in the target tissues and we characterize the kinetics of
394 its distribution. The study was designed to address a knowledge gap and a methodological gap. Indeed,
395 one of the most challenging issues in environmental toxicity is to understand and model long-
396 term/low-dose effects (Barouki, 2010). Concerning POPs, such long-term effects are usually explained
397 by continuous exposure due to the persistence and bioaccumulation of those pollutants in the
398 environment and by continuous release from internal storage sites such as the AT. It was not clear
399 whether release from the AT was significant and whether it could induce biological or toxic effects in
400 other tissues. Evidence for the latter mechanism has been gathered indirectly for example by studying
401 weight loss in obese humans (Kim et al., 2011). The present study addresses specifically this point and
402 provides direct evidence for the release of a POP from AT and describes its effects on other tissues.
403 Thus, release of POPs from AT is likely to play a significant role in long-term effects of pollutants.

404 In order to study the release of POPs from the AT and its properties, we developed an adequate
405 experimental model based on grafting of AT from a contaminated animal into a non-contaminated
406 one. It explores the effects of a continuous release from an internal compartment, the AT and reflects
407 exposures of humans and animals to POPs. Other models of continuous release do exist such as release
408 capsules which have been designed mostly for pharmacological purposes (i.e. treatment of chronic
409 pain) or micro-osmotic pumps (Mercadante, 2017; Tauer et al, 2013); however, both models differ
410 from our model in the nature of the delivery compartment which is biologically relevant in our case
411 and includes adipocytes, endothelial and immune cells which could influence the release. In that sense,
412 the model described here is a better representation of the actual internal exposure than artificial
413 models. However, it has its limitations too in that the graft could undergo different stresses and
414 outcomes such a fibrosis or altered vascularization which may influence the observed results.

415 This AT graft model is clearly complementary to more traditional exposure models through
416 ingestion or injection. It is not meant to be an alternative to other models but rather to identify the
417 contributions of internal sources as compared to external exposures. In that sense it can help in
418 assessing long-term effects even after withdrawal of external exposures. The model also allows the
419 derivation of relevant toxicokinetic and toxicodynamic features that are complementary to those
420 derived from classical drug treatment regimens.

421 Our experimental data improve the confidence in the PBPK model for mice that was developed
422 previously (USEPA, 2012), and adapted for the present work. The intraperitoneal exposures to 1, 10

1417
1418
1419
1420
1421
1422
1423
1424
1425
1426
1427
1428
1429
1430
1431
1432
1433
1434
1435
1436
1437
1438
1439
1440
1441
1442
1443
1444
1445
1446
1447
1448
1449
1450
1451
1452
1453
1454
1455
1456
1457
1458
1459
1460
1461
1462
1463
1464
1465
1466
1467
1468
1469
1470
1471
1472
1473
1474
1475

423 and 25 $\mu\text{g.kg}^{-1}$ of body weight were also modeled (SFigure 4, Suppl. Mat.). The model accurately
424 reproduces the experimental measurements, 48 hours following the single intraperitoneal
425 administration for all doses, regarding the ratio of doses and the amount measured in tissues (Equation
426 1). Yet, the model has its limitations since it requires surgery and some of the effects could be biased
427 by the fate of the graft. Indeed, we observed individual differences in vascularization or fibrosis, which
428 could impact TCDD release from the graft. These observations could partly explain why between 4 to
429 10 weeks, the slope of TCDD elimination from the graft, changes (Figure 3); a better characterization
430 of the vascularization of the graft will be necessary for our on-going projects. We believe that besides
431 the structural variabilities described previously, metabolic adaptations and heterogenous lipid content
432 could also influence TCDD release. A better characterization of the graft would improve the description
433 of the PBPK model. However, at this point, it predicts with accuracy the evolution of TCDD
434 concentrations in both AT and liver known as the most important depository organs of this pollutant
435 in mammals. Indeed, our experimental data that match the PBPK model, indicate that despite some
436 variability in the initial concentrations of TCDD in the graft (mean of $4815 \pm 2122 \mu\text{g.kg}^{-1}$), the POP
437 diffuses to other key organs such as the host AT, liver or brain following different kinetics. The release
438 of TCDD from the graft is relatively rapid with a half-life of 1.03 weeks ($\cong 173$ hours, from weeks 0-4)
439 and 5.53 weeks (932 hours from week 4), suggesting that after 10 weeks, more than 97% has been
440 released from the graft. The modeled kinetics of release and distribution is in line with the
441 experimental data (Figure 3); this simulation represents an exciting predictive tool which also could be
442 improved in the future using a wider range of POPs and representative mixtures.

443
444 The release of TCDD influences important biological pathways that are involved in liver and AT
445 dysfunction. For this part of the work, the focus was first on xenobiotic metabolizing enzymes
446 (biomarkers of an activated AhR signaling pathway) and inflammatory cytokines/chemokines which
447 are classically induced upon TCDD exposure. As expected (regarding the distribution of TCDD), the AhR-
448 target genes (CYP1A1, CYP1B1, PAI-1) were significantly induced at the mRNA levels in the liver and AT
449 3 weeks following grafting (Tables 1 and 2). Similarly, an inflammatory signature is observed in both
450 tissues which is in line with the literature and our former studies using traditional modes of exposure
451 (Duval *et al.* 2017; Kim *et al.* 2011, 2012). Furthermore, a highly significant increase of the expression
452 of two biomarkers of fibrosis in the liver (alpha-Smooth Muscle Action or alpha-SMA and collagen 1A1
453 or COL1A1IL) was obtained, confirming our recent observations on the occurrence of liver fibrosis
454 following exposure to TCDD (Duval *et al.* 2017). Finally, the mRNA expression of the three key
455 gluconeogenic enzymes, pyruvate carboxylase (PC), cytosolic phosphoenolpyruvate carboxykinase
456 (PEPCK), glucose 6-phosphatase (G6Pase) showed significant inductions. Such enzymes contribute to
457 the maintenance of glycemia during fasting, but their induction is also classically described in type 2

1476
1477
1478
1479
1480
1481
1482
1483
1484
1485
1486
1487
1488
1489
1490
1491
1492
1493
1494
1495
1496
1497
1498
1499
1500
1501
1502
1503
1504
1505
1506
1507
1508
1509
1510
1511
1512
1513
1514
1515
1516
1517
1518
1519
1520
1521
1522
1523
1524
1525
1526
1527
1528
1529
1530
1531
1532
1533
1534

457 diabetes (Beale *et al.*, 2007). These results are different from those of other teams who reported that
458 expression of PEPCK is strongly repressed by TCDD; in 1993, Stahl *and coll.* demonstrated that TCDD
459 exposure decreased hepatic gluconeogenesis due to a reduction of PEPCK activity and mRNA
460 expression (Stahl *et al.*, 1993) which has been also observed in another model by Dunlap *and coll*
461 (Dunlap *et al.*, 2002). This was also demonstrated for PC following a short treatment in hepatic rat
462 livers (Ilian *et al.*, 1996). We hypothesize that the difference between those observations and our data
463 is due to the mode of exposure; most previous experiments were performed using an acute-based
464 exposure protocol while our model allows a constant delivery of TCDD for several weeks. While we are
465 not able at this point to explain mechanistically the differences, we think that a sustained low-dose
466 delivery of TCDD could have a different impact than an acute delivery of TCDD, on the regulation of
467 gluconeogenesis enzymes.

468 This observation suggests that a continuous exposure of TCDD could disrupt carbohydrate and
469 lipid metabolism and, more generally, liver functions. Thus, the TCDD released from an internal storage
470 site can induce gene expression changes in at least two tissues that reflect biological activity of this
471 pollutant and which is in line with what is known about its toxicity. While it is likely that some of the
472 effects of TCDD on gene expression are related to the activation of the AhR pathway (such as the
473 induction of CYP1 genes), other effects may be indirect. For example, TCDD and the AhR activate the
474 expression of inflammatory cytokines through direct or indirect, genomic or non-genomic pathways
475 (Kim *et al.* 2012), and those cytokines could also be responsible for the other genomic alterations
476 observed in the liver and the AT; moreover, as the release of TCDD from the graft is relatively rapid
477 and then high, these gene expressions could represent an adaptive response to a major environmental
478 stress (a high dose of TCDD). In order to delineate the actual mechanisms involved in the effects of
479 contaminated/xenografted-AT on gene expression in distant tissues after such periods of exposure (3
480 weeks in our case), additional studies would be required. Thus, we can conclude that the release of
481 POPs from internal storage sites could play a significant role in the toxicity of those pollutants that
482 needs to be further investigated using a wider range of POPs and representative mixtures.

483
484 **7. Conclusion**

485 The experimental model described here represents a novel approach to explore exposure to
486 pollutants from endogenous sources and their long-term toxicities. It is meant to be complementary
487 to other experimental protocols of exposure through diet, dermal, intraperitoneal injection or gavage
488 procedures.

1535
1536
1537
1538
1539
1540
1541
1542
1543
1544
1545
1546
1547
1548
1549
1550
1551
1552
1553
1554
1555
1556
1557
1558
1559
1560
1561
1562
1563
1564
1565
1566
1567
1568
1569
1570
1571
1572
1573
1574
1575
1576
1577
1578
1579
1580
1581
1582
1583
1584
1585
1586
1587
1588
1589
1590
1591
1592
1593

490 8. References

- 491 Ambolet-Camoit, A., Ottolenghi, C., Leblanc, A., Kim, M-J., Letourneur, F., Jacques, S., Cagnard, N.,
492 Guguen-Guillouzo, C., Barouki, R., Aggerbeck, M., 2015. Two persistent organic pollutants
493 which act through different xenosensors (alpha-endosulfan and 2,3,7,8 tetrachlorodibenzo-p-
494 dioxin) interact in a mixture and downregulate multiple genes involved in human hepatocyte
495 lipid and glucose metabolism. *Biochimie* 116, 79-91.
- 496 Barouki, R., 2010. Linking long-term toxicity of xeno-chemicals with short-term biological adaptation.
497 *Biochimie* 92, 1222-1226. <https://doi.org/10.1016/j.biochi.2010.02.026>
- 498 Beale, E.G., Harvey, B.J., Forest, C., 2007. PCK1 and PCK2 as candidate diabetes and obesity genes. *Cell*
499 *Biochem. Biophys.* 48, 89-95.
- 500 Birnbaum, L.S., 1995. Developmental effects of dioxins. *Environ. Health Perspect.* 103 Suppl 7, 89-94.
- 501 Boffetta, P., Mundt, K.A., Adami, H-O., Cole, P., Mandel, J.S., 2011. TCDD and cancer: a critical review
502 of epidemiologic studies. *Crit. Rev. Toxicol.* 41, 7, 622-636.
- 503 Bonde, J.S., Flachs, E.M., Rimborg, S., Glazer, C.H., Giwercman, A., 2016. The epidemiologic evidence
504 linking prenatal and postnatal exposure to endocrine disrupting chemicals with male
505 reproductive disorders: a systematic review and meta-analysis. *Hum. Reprod. Update.* 23, 104-
506 125.
- 507 Brown, R.P., Delp, M.D., Lindstedt, S.L., Rhomberg, L.R., Beliles, R.P., 1997. Physiological Parameter
508 Values for Physiologically Based Pharmacokinetic Models. *Toxicol. Ind. Health* 13, 407-484.
509 <https://doi.org/10.1177/074823379701300401>
- 510 Carrier, G., 1995. Modeling of the Toxicokinetics of Polychlorinated Dibenzo-p-dioxins and
511 Dibenzofurans in Mammals, Including Humans I. Nonlinear Distribution of PCDD/PCDF Body
512 Burden between Liver and Adipose Tissues. *Toxicol. Appl. Pharmacol.* 131, 253-266.
513 <https://doi.org/10.1006/taap.1995.1068>
- 514 Chevrier, J., Dewailly, E., Ayotte, P., Mauriège, P., Després, J.P., Tremblay, A., 2000. Body weight loss
515 increases plasma and adipose tissue concentrations of potentially toxic pollutants in obese
516 individuals. *Int J Obes Relat Metab Disord.* 24, 10, 1272-8.
- 517 Costera, A., Feidt, C., Marchand, P., Le Bizec, B., Rychen, G., 2006. PCDD/F and PCB transfer to milk in
518 goats exposed to a long-term intake of contaminated hay. *Chemosphere.* 64, 4, 650-657.
- 519 Diliberto, J.J., Burgin, D., Birnbaum, L.S., 1997. Role of CYP1A2 in hepatic sequestration of dioxin:

1594
1595
1596 520 studies using CYP1A2 knock-out mice. *Biochem. Biophys. Res. Commun.* 236, 431–433.
1597
1598 521 <https://doi.org/10.1006/bbrc.1997.6973>
1599
1600 522 Dunlap, D.Y., Ikeda, I., Nagashima, H., Vogel, C.F., Matsumura, F, 2002. Effects of src-deficiency on the
1601 expression of in vivo toxicity of TCDD in a strain of c-src knockout mice procured through six
1602 523 generations of backcrossings to C57BL/6 mice. *Toxicology.* 172, 125-41.
1603 524
1604
1605 525 Duval, C., Teixeira-Clerc, F., Leblanc, A.F., Touch, S., Emond, C., Guerre-Millo, M., Lotersztajn, S.,
1606 526 Barouki, R., Aggerbeck, M., Coumoul, X., 2017. Chronic Exposure to Low Doses of Dioxin
1608 527 Promotes Liver Fibrosis Development in the C57BL/6J Diet-Induced Obesity Mouse Model.
1609 *Environ Health Perspect.* 125, 428-436.
1610 528
1611
1612 529 Emond, C., 2004. Physiologically Based Pharmacokinetic Model for Developmental Exposures to TCDD
1613 in the Rat. *Toxicol. Sci.* 80, 115–133. <https://doi.org/10.1093/toxsci/kfh117>
1614 530
1615
1616 531 Emond, C., Birnbaum, L.S., DeVito, M.J., 2006. Use of a physiologically based pharmacokinetic model
1617 532 for rats to study the influence of body fat mass and induction of CYP1A2 on the
1618 pharmacokinetics of TCDD. *Environ. Health Perspect.* 114, 1394–1400.
1619 533
1620
1621 534 Emond, C., DeVito, M.J., Diliberto, J.J., Birnbaum, L.S., 2018. The Influence of Obesity on the
1622 535 Pharmacokinetics of Dioxin in Mice: An Assessment Using Classical and PBPK Modeling.
1624 536 *Toxicol. Sci.* <https://doi.org/10.1093/toxsci/kfy078>
1625
1626 537 Emond, C., Michalek, J.E., Birnbaum, L.S., DeVito, M.J., 2005. Comparison of the use of a physiologically
1627 538 based pharmacokinetic model and a classical pharmacokinetic model for dioxin exposure
1629 539 assessments. *Environ. Health Perspect.* 113, 1666–1668.
1630
1631
1632 540 Emond, C., Ruiz, P., Mumtaz, M., 2017. Physiologically based pharmacokinetic toolkit to evaluate
1633 541 environmental exposures: Applications of the dioxin model to study real life exposures.
1634 *Toxicol. Appl. Pharmacol.* 315, 70–79. <https://doi.org/10.1016/j.taap.2016.12.007>
1635 542
1636
1637 543 Emond, C., DeVito, M., Warner, M., Eskenazi, B., Mocarelli, P., Birnbaum, L.S., 2016. An assessment of
1638 544 dioxin exposure across gestation and lactation using a PBPK model and new data from Seveso.
1639 *Environ Int.* 92-93, 23-32.
1640 545
1641
1642 546 Emond, C., Raymer, J.H., Studabaker, W.B., Garner, C.E., Birnbaum, L.S., 2010. A physiologically based
1643 547 pharmacokinetic model for developmental exposure to BDE-47 in rats. *Toxicol Appl*
1645 548 *Pharmacol.* 242, 290-8.
1646
1647 549 Gasiewicz, T.A., Geiger, L.E., Rucci, G., Neal, R.A., 1983. Distribution, excretion, and metabolism of
1648 550 2,3,7,8-tetrachlorodibenzo-p-dioxin in C57BL/6J, DBA/2J, and B6D2F1/J mice. *Drug Metab.*

1653
1654
1655 551 Dispos. Biol. Fate Chem. 11, 397–403.
1656
1657 552 Goodman, M., Narayan, K.M.V., Flanders, D., Chang, E.T., Adami, H-O., Boffetta, P., Mandel, J.S., 2015.
1658
1659 553 Dose-Response Relationship Between Serum 2,3,7,8-Tetrachlorodibenzo-p-Dioxin and
1660
1661 554 Diabetes Mellitus: A Meta-Analysis. American Journal of Epidemiology. 181, 6, 374.
1662
1663 555 Guyot, E., Chevallier, A., Barouki, R., Coumoul, X., 2013. The AhR twist: ligand-dependent AhR signaling
1664 556 and pharmaco-toxicological implications. Drug Discov. Today. 18, 479-486.
1665
1666 557 Ilian, M.A., Sparrow, B.R., Ryu, B.W., Selivonchick, D.P., Schaup, H.W., 1996. Expression of
1667
1668 558 hepatic pyruvate carboxylase mRNA in C57BL/6J Ah(b/b) and congenic Ah((d/d)) mice exposed
1669
1670 559 to 2,3,7,8-tetrachlorodibenzo-p-dioxin. J Biochem Toxicol. 11, 51-6.
1671
1672 560 Imbeault, P., Chevrier, J., Dewailly, E., Ayotte, P., Després, J.P., Mauriège, P., Tremblay, A, 2002.
1673 561 Increase in plasma pollutant levels in response to weight loss is associated with the reduction
1674
1675 562 of fasting insulin levels in men but not in women. Metabolism. 51, 4, 482-6.
1676
1677 563 Juricek, L., Bui, L.-C., Busi, F., Pierre, S., Guyot, E., Lamouri, A., Dupret, J.-M., Barouki, R., Coumoul, X.,
1678
1679 564 Rodrigues-Lima, F., 2014. Activation of the aryl hydrocarbon receptor by carcinogenic aromatic
1680 565 amines and modulatory effects of their N-acetylated metabolites. Arch. Toxicol.
1681
1682 566 <https://doi.org/10.1007/s00204-014-1367-7>
1683
1684 567 Kim, M.-J., Marchand, P., Henegar, C., Antignac, J.-P., Alili, R., Poitou, C., Bouillot, J.-L., Basdevant, A.,
1685 568 Le Bizec, B., Barouki, R., Clément, K., 2011. Fate and complex pathogenic effects of dioxins and
1686
1687 569 polychlorinated biphenyls in obese subjects before and after drastic weight loss. Environ.
1688
1689 570 Health Perspect. 119, 377–383. <https://doi.org/10.1289/ehp.1002848>
1690
1691 571 Kim, M.-J., Pelloux, V., Guyot, E., Tordjman, J., Bui, L.-C., Chevallier, A., Forest, C., Benelli, C., Clément,
1692 572 K., Barouki, R., 2012. Inflammatory pathway genes belong to major targets of persistent
1693
1694 573 organic pollutants in adipose cells. Environ. Health Perspect. 120, 508-514.
1695
1696 574 Kissel, J.C., Robarge, G.M., 1998. Assessing the elimination of 2,3,7,8-TCDD from humans with a
1697 575 physiologically based pharmacokinetic model. Chemosphere 17, 2017–2027.
1698
1699 576 [https://doi.org/10.1016/0045-6535\(88\)90012-4](https://doi.org/10.1016/0045-6535(88)90012-4)
1700
1701 577 La Merrill, M., Emond, C., Kim, M.-J., Antignac, J.-P., Le Bizec, B., Clement, K., Birnbaum, L.S., Barouki, R
1702
1703 578 2013. Toxicological function of adipose tissue: focus on persistent organic pollutants. Environ.
1704 579 Health Perspect. 121, 162-169.
1705
1706 580 Lee, Y.M., Kim, K.S., Jacobs, D.R., Lee, D.H., 2017. Persistent organic pollutants in adipose tissue should
1707
1708 581 be considered in obesity research. Obes Rev 18, 2, 129-139.
1709
1710
1711

1712
1713
1714 582 Leung, H., Ku, R.H., Paustenbach, D.J., Andersen, M.E., 1988. A physiologically based pharmacokinetic
1715
1716 583 model for 2,3,7,8-tetrachlorodibenzo-p-dioxin in C57BL/6J and DBA/2J mice. *Toxicol Lett* 42,
1717 584 15-28.
1718
1719 585 Leung, H., Paustenbach, D.J., Murray, F., Andersen, M.E., 1990. A physiological pharmacokinetic
1720 586 description of the tissue distribution and enzyme-inducing properties of 2,3,7,8-
1721 587 tetrachlorodibenzo-p-dioxin in the rat. *Toxicol Appl Pharmacol* 103, 399-410.
1722
1723
1724 588 Mercadante, S., 2017. Oxycodone extended release capsules for the treatment of chronic pain. *Expert*
1725 589 *Rev Neurother.* 17, 427-431
1726
1727
1728 590 Mostafalou, S., 2016. Persistent Organic Pollutants and Concern Over the Link with Insulin Resistance
1729 591 Related Metabolic Diseases. *Rev Environ Contam Toxicol* 238, 69-89.
1730
1731
1732 592 Novelli, M., Piaggi, S., De Tata, V., 2005. 2,3,7,8-Tetrachlorodibenzo-p-dioxin-induced impairment of
1733 593 glucose-stimulated insulin secretion in isolated rat pancreatic islets. *Toxicol. Lett.* 156, 2, 307-
1734 594 314.
1735
1736
1737 595 Pfaffl, M.W., 2001. A new mathematical model for relative quantification in real-time RT-PCR. *Nucleic*
1738 596 *Acids Res.* 29, e45.
1739
1740
1741 597 Smarr, M.M., Kannan, K., Buck Louis, G.M., 2016. Endocrine disrupting chemicals and endometriosis.
1742 598 *Fertility and Sterility* 106, 4, 959-966.
1743
1744
1745 599 Stahl, B.U., Beer, D.G., Weber, L.W., Rozman, K., 1993. Reduction of hepatic phosphoenolpyruvate
1746 600 carboxykinase (PEPCK) activity by 2,3,7,8-tetrachlorodibenzo-p-dioxin (TCDD) is due to
1747 601 decreased mRNA levels. *Toxicology.* 79, 81-95.
1748
1749
1750 602 Tauer, J.T., Hofbauer, L.C., Jung, R., Erben, R.G., Suttorp, M., 2013. Micro-osmotic pumps for
1751 603 continuous release of the tyrosine kinase inhibitor bosutinib in juvenile rats and its impact on
1752 604 bone growth. *Med Sci Monit Basic Res.* 19, 274-8.
1753
1754
1755 605 USEPA, 2012. EPA's reanalysis of key issues related to dioxin toxicity and response to NAS comments,
1756 606 in: (EPA/600/R-10/038F), (EPA/600/R-10/038F).
1757
1758
1759 607 Wang, X., Santostefano, M.J., Evans, M.V., Richardson, V.M., Diliberto, J.J., Birnbaum, L.S., 1997.
1760 608 Determination of Parameters Responsible for Pharmacokinetic Behavior of TCDD in Female
1761 609 Sprague-Dawley Rats. *Toxicol. Appl. Pharmacol.* 147, 151-168.
1762
1763 610 <https://doi.org/10.1006/taap.1997.8242>
1764
1765
1766 611 White, S.S., Birnbaum, L.S., 2009. An overview of the effects of dioxins and dioxin-like compounds on
1767
1768
1769
1770

1771
1772
1773 612 vertebrates, as documented in human and ecological epidemiology. *J. Environ. Sci. Health Part*
1774 *C Environ. Carcinog. Ecotoxicol. Rev.* 27, 197-211.
1775 613
1776 614 <https://doi.org/10.1080/10590500903310047>
1777
1778 615 Wolfe, W.H., Michalek, J.E., Miner, J.C., Pirkle, J.L., Caudill, S.P., Patterson, D.G., Needham, L.L., 1994.
1779
1780 616 Determinants of TCDD half-life in veterans of operation ranch hand. *J. Toxicol. Environ. Health*
1781
1782 617 41, 481-488. <https://doi.org/10.1080/15287399409531858>
1783
1784 618
1785
1786 619
1787
1788 620
1789
1790
1791
1792
1793
1794
1795
1796
1797
1798
1799
1800
1801
1802
1803
1804
1805
1806
1807
1808
1809
1810
1811
1812
1813
1814
1815
1816
1817
1818
1819
1820
1821
1822
1823
1824
1825
1826
1827
1828
1829